Material and Methods
A549 (NSCLC) and 143B (osteosarcoma) were depleted from their mtDNA (ρ°) via ethidium bromide exposure. Cytoplasmic hybrids (cybrids) were produced by fusing the 143B-ρ° cell line with mtDNA derived from fibroblasts carrying an m.3243A>G mutation. All cells were metabolically characterized using the Seahorse XF96 analyzer. Pharmacological OXPHOS inhibition was induced by either metformin or rotenone. CAIX, VEGF, HIF-1α and PHD2 mRNA expression upon hypoxia (0.2%, 16h) was determined by qPCR. CAIX and HIF-1α protein levels were determined by Western blotting. Reactive oxygen species levels (ROS) were measured using DHR flow cytometry. Tumor growth and hypoxic fraction (pimonidazole positivity) was monitored for xenografts generated from the cytoplasmic hybrids.
Results
Reduced ($p<0.05$) mitochondrial respiration and an increased glucose metabolism were observed in ρ° cell lines (<6% remaining mtDNA copy number) and in the cybrid cell lines (point mutation >94.5%). Upon hypoxia, OXPHOS inhibition resulted in decreased ($p<0.05$) CAIX (protein/mRNA), VEGF (mRNA) and HIF-1α (protein) expression levels. ROS and PHD2 levels could not explain these observations. Similar results were found upon pharmacological inhibition. In vivo, tumor take (>50 mm^3) took longer for cybrid xenografts, but growth rates were similar compared to control tumors once established. Previously, it has been shown that HIF-1α is responsible for tumor establishment. In agreement, HIF-1α expression levels and the pimonidazole-positive hypoxic fraction were reduced for the cybrid xenografts. Most of the tumors established from the mutant cell line lost their m.3243A>G mutation in vivo, possibly explaining the delayed tumor take and the absence of an effect on growth rate. The presence of HIF-1α in cell lines with lower mutation percentage supports this observation.
Conclusion
Our results demonstrated that OXPHOS inhibition leads to a decreased HIF-1α stabilization and expression of downstream targets such as CAIX, VEGF and a reduced hypoxic fraction in vivo. Inhibition of mitochondrial function is therefore an interesting approach to increase therapeutic efficacy for radiation of hypoxic tumors.

EP-2330 MRI based high precision irradiation of a pancreatic tumor using SARRP: a treatment planning study
S. Dobiasch[1,2], S. Kampfer[1,3], D. Schilling[1,4], J.J. Wilkens[1,3,4], S.E. Combs[1,2,4]
[1]*Klinikum rechts der Isar- TU München, Department of Radiation Oncology, München, Germany*
[2]*Deutsches Konsortium für Translationale Krebsforschung DKTK, Partner Site Munich, Munich, Germany*
[3]*Technical University of Munich TUM, Physics Department, Garching, Germany*
[4]*Institute of Innovative Radiotherapy iRT, Department of Radiation Sciences DRS, Neuherberg, Germany*

Purpose or Objective
Only recently, imaging and high-precision radiation devices for preclinical tumor mouse models have been developed. Image guided radiation therapy (IGRT) including innovative treatment planning techniques comparable to patients' treatment can be achieved in a translational context.
The present study aims to evaluate different treatment techniques and collimator shapes in planning related settings (contouring, fusion) for high-precision radiation therapy (RT) of an orthotopic pancreatic tumor mouse model.
Material and Methods
In an orthotopic pancreatic cancer model MRI-based radiation treatment planning was established. Two advanced radiation techniques (rotation and 3-dimensional multifield RT) were performed and depending on the tumor volume different collimators (fixed sizes and variable) were used for subsequent irradiation with the SARRP system (Small Animal Radiation Research Platform, Xstrahl Ltd). Dose distributions in gross tumor volume (GTV) and organs at risk (OAR) were analyzed and compared for each treatment setting.
Results
Magnetic resonance imaging (MRI) detects gross tumor volume and organs at risk with improved soft tissue contrast. MRI-based 3D treatment planning allows an optimal sparing of normal tissue and maximum dose in the GTV, thus providing a perfect basis for an improved imaging in high-precision RT. All advanced radiation techniques (rotation and multifield) established in a preclinical tumor mouse model reflect clinical treatment plans of pancreatic cancer patients.
Conclusion
A MRI-based treatment planning and image guided high-precision RT using different innovative radiation techniques was established in an orthotopic pancreatic tumor mouse model. The development of variable collimators in preclinical settings allows considering surrounding safety margins, perfect coverage of GTV, more flexibility of tumor shapes and optimal reflecting the clinical setting.

EP-2331 Tumor microenvironment modifications recorded with IVIM perfusion analysis after radiotherapy.
F. Lallemand[1], N. Leroi[2], M. Bahri[3], E. Balteau[3], A. Noël[2], P. Coucke[1], A. Plenevaux[3], P. Martinive[1]
[1]*CHU de Liège, Department of Radiotherapy-Oncology, Liège, Belgium*
[2]*ULg, Laboratory of Tumor and Development Biology, Liège, Belgium*
[3]*ULg, Cyclotron Research Centre, Liège, Belgium*

Purpose or Objective
Neoadjuvant radiotherapy (NeoRT) improves tumor local control and facilitates tumor resection in many cancers. The timing between the end of the NeoRT and surgery is driven by the occurrence of side effects or the tumor downsizing. Some clinical studies demonstrated that the timing of surgery and the RT schedule influence tumor dissemination and subsequently patient overall survival (acta oncol 2006). Previously, we developed a pre-clinical model demonstrating an impact of NeoRT schedule and the timing of surgery on metastatic spreading (Oncotarget 2015). Here, we used functional MRI (fMRI) to record tumor microenvironment modifications after NeoRT. We aim to get non-invasive markers to establish the best timing to perform surgery and avoiding tumor spreading.
Material and Methods
Based on our NeoRT model, MDA-MB 231 and 4T1 cells were implanted in the flank of SCID and BalbC mice, respectively. We locally irradiated (PXI, X-Rad SmART) tumors with 2x5Gy and then surgically removed at different time points after RT. We acquired fMRI (9,4T Agilent) before and after RT. Diffusion Weighted (DW) - MRI was performed every 2 days between RT and surgery.

For each tumor, we acquired 8 slices of 1 mm thickness and 0.5 mm gap with an "in plane voxel resolution" of 0.5 mm. For DW-MRI, we performed FSEMS (Fast Spin Echo MultiSlice) sequences, with 9 different B-value (from 40 to 1000) and B0, in the 3 main directions. We performed IVIM (IntraVoxel Incoherent Motion) analysis to obtain information on intravascular diffusion, related to perfusion (F: perfusion factor) and subsequently tumor vessels perfusion.

Results

With the MDA-MB 231, we observed a significant and transient increase (60% of the basal value (n=6, p<0,05)) of F and D* parameters related to perfusion. The other parameters of the DW-MRI, ADC and D presented no modification. We observed similar results with 4T1 cells, where F increased at day 3 (55% of the basal value, n=10, p<0,05) then returned to initial level. The difference in timing for the peak of F (day 6 vs day 3) could be related to the difference in tumor growth according to the cell line (four weeks for MDA-MB 231 cells vs one week for 4T1 cells). We also observed a decrease of hypoxia (pimonidazole staining) when surgery was performed on the peak but vascular architecture was not affected. Moreover, performing surgery during F and D* peak, in the MDA-MB 231model, is associated with an increase of lung metastases: 115% and 187% compared to a surgery performed before or after the peak.

Conclusion

We demonstrated the feasibility of repetitive fMRI imaging in preclinical models after NeoRT. We showed a significant difference in perfusion-related parameters (D* and F) at a specific time point depending of tumor cells correlated with tumor metastases. We demonstrated the feasibility of Image Guided Surgery for decreasing tumor metastases after NeoRT.

EP-2332 A concept to personalize radiation oncology: Predicting cell-specific survival prior to treatment

H. Oesten[1,2], C. Von Neubeck[1,3], S. Löck[1,3,4], W. Enghardt[1,2,4], M. Krause[1,2,3,4,5], S. McMahon[6], C. Grassberger[7], H. Paganetti[7], A. Lühr[1,2,3]

[1]OncoRay - National Center for Radiation Research in Oncology, Faculty of Medicine and University Hospital Carl Gustav Carus- Technische Universität Dresden- Dresden- Helmholtz - Zentrum Dresden - Rossendorf, Dresden, Germany

[2]Helmholtz - Zentrum Dresden - Rossendorf HZDR, Institute of Radiooncology - OncoRay, Dresden, Germany

[3]German Cancer Consortium DKTK- partner site Dresden, German Cancer Research Center DKFZ, Heidelberg, Germany

[4]Department of Radiation Oncology, Faculty of Medicine and University Hospital Carl Gustav Carus- Technische Universität Dresden, Dresden, Germany

[5]National Center for Tumor Diseases, partner site, Dresden, Germany

[6]Centre for Cancer Research and Cell Biology, Radiation Biology Group, Belfast, Ireland

[7]Massachusetts General Hospital and Harvard Medical School, Department of Radiation Oncology, Boston, USA

Purpose or Objective

To enhance tumor response and thus treatment outcome in radiation therapy, a dose prescription strategy is necessary to individualize radiation oncology. However, prediction of cell-specific survival prior to treatment is currently unavailable. Thus, we developed an approach to stratify patients by predicting individual radiation response based on cell survival.

Material and Methods

Based on a previously developed mechanistic radiation response model of DNA repair and cell survival (CS) prediction for normal tissue cells, we simulated measured radiobiological parameters (α and ß) of 19 in vitro cancer cell lines (skin, lung, brain). The radiation model incorporated four cell-specific parameters: number of chromosomes, p53 mutation status, cell-cycle distribution and the effective genome size (GS). Only the first three input parameters were experimentally available; the latter was obtained by minimizing the difference between the simulated and measured α and ß values. A parametrization of the GS as a function of the cells' chromosome number and nucleus volume was proposed. The use of these input parameters was validated by comparing the simulated outcome of time-dependent γH2AX data over 24h with independent experimental datasets.

Results

Overall good agreement between simulated and measured in vitro cancer CS curves was achieved (Fig. 1). The measured ß values increased quadratically with the obtained GS (R^2=0.81) irrespective of other cell-specific parameters (Fig. 2b). The measured α values increased linearly with GS manifesting different slopes distinguishable into the cells' p53 mutation status (Fig. 2a). Measured α and ß values were predictable based on GS with a one-sigma uncertainty: σ=0.04Gy^{-1} for α and σ=0.01Gy^{-2} for ß. The GS correlated (R^2=0.70) with the number of chromosomes for all but four cell lines. The detailed cell-specific cell cycle distribution had a negligible impact on α and ß. Measured time-dependent γH2AX data were consistent with the repair kinetics simulations (R^2=0.95).

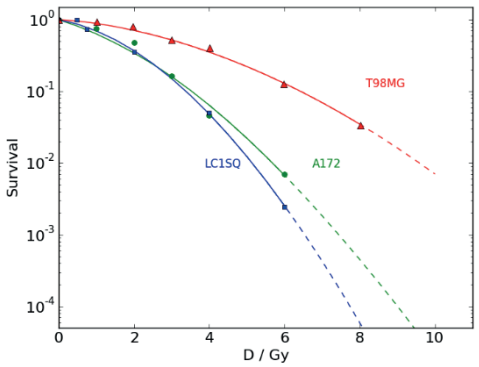

Fig.1: Measured (symbols) and simulated (lines) survival curves for 3 cancer cell lines (green: A172 (p53^{wt}), red: T98MG (p53^{mt}), blue: LC1SQ (p53^{mt})); highlighted in Fig.2

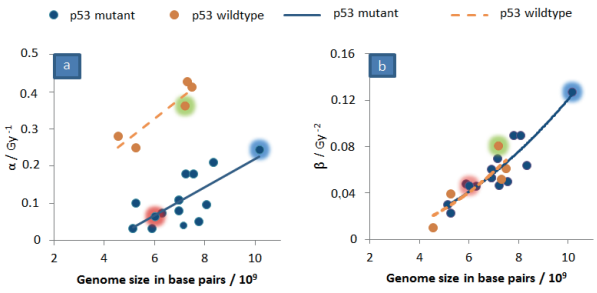

Fig.2: Measured α and ß values as a function of simulated genome size: **a)** α increases linearly with genome size and can be stratified in two groups: p53^{wt}, p53^{mt}; **b)** ß increases quadratically with genome size for all two groups. Highlight: see Fig.1